Experimental Validation of the Real-Time Control of an Electric-Vehicle Charging Station

Roman Rudnik
Jean-Yves Le Boudec
Laboratory for Communications and Applications 2
École Polytechnique Fédérale de Lausanne
Lausanne, Switzerland
{roman.rudnik, jean-yves.leboudec}@epfl.ch

Sherif Fahmy
Mario Paolone
Distributed Electrical Systems Laboratory
École Polytechnique Fédérale de Lausanne
Lausanne, Switzerland
{sherif.fahmy, mario.paolone}@epfl.ch

2021 IEEE Madrid PowerTech | 978-1-6654-3597-0/21/$31.00 ©2021 IEEE | DOI: 10.1109/PowerTech46648.2021.9495070

***Abstract*—The high penetration of electric vehicles (EVs) charging stations (CSs), together with the progressive availability of distributed energy resources, increases the risk of grid overloading and power-quality degradation. Real-time control has been advocated by the recent literature as an alternative to costly grid reinforcement. Performance of most of the existing control methods is assessed via simulations, and real-field validation is rarely performed. We present the experimental validation of a recently proposed real-time control method for EVs CS. This method works at sub-second scale and allows the CS to adapt to the rapidly changing state of the grid caused by highly volatile energy resources, such as photo-voltaic (PV) plants. The method fairly allocates the available power, proportional to the EVs needs, while minimizing the EVs battery wear due to frequent charging power variations. It tracks an aggregated power-setpoint that comes from the main grid controller by solving a mixed-integer optimization problem. Our main goal is to show that the method works in the field, i.e., it can control the charge of commercial EVs that are connected to a real grid through a CS. The field validation has two challenges. The first one is to study the real-time capabilities of the method and by analysing how fast it computes the control power-setpoints. The second one refers to the handling of the non-ideal response of EVs to the control power-setpoints due to implementation and reaction delays and inaccuracies. The experimental results demonstrate the performance of the method and show that it can be deployed in the field.**

***Index Terms*—Electric vehicles, real-time control.**

I. Introduction

The significant integration of electric vehicles (EVs) charging stations (CSs) has started to influence the power grid operation. The deployment of CSs, together with the presence of distributed renewable-energy resources, such as photo-voltaic plants (PVs), increases the risk of a large power-quality degradation, i.e., line congestions, voltage violations, and transformer overrating [1]. Instead of traditional grid reinforcement, real-time control can be used as an alternative to better exploit the grid power transfer capability [2]. For example, assume that a distribution grid contains local generation (e.g., PV plants) and EV CSs, both connected to the main grid through a transformer. In such a setup, EVs are expected to be mostly charged by the PV production in order to reduce their CO_2 footprint. Additionally, the presence of other loads (e.g., domestic building) together with CS consumption may cause line congestions or transformer overrating during peak hours. As a consequence, the EVs must follow a possible rapid fluctuation of the PV production, while satisfying the distribution grid constraints. In this case, the real-time control is able to maximally use the limited resources of the grid to charge EVs, while keeping the grid in a feasible state.

The charging control of EVs has been extensively exploited in the literature in order to provide ancillary services [3]–[6]. However, the validation of most of the methods for the charging control of EVs relies on simulations. Due to its technical difficulty, the real-field experimental validation is rarely performed. The authors in [7]–[9] experimentally validated a droop-based charging-control method for the provision of ancillary services, such as frequency control, voltage control and congestion management. However, the EVs are controlled without accounting for their charging requirements, i.e., the energy demands and expected charging times. In this same direction, we report the field validation of the real-time EVs charging control recently proposed in [10]. The method has following features: (i) it tracks an aggregated power-setpoint dictated by a grid controller to the CS, (ii) it minimizes the battery wear of every EV and (iii) it fairly allocates the power to EVs. In order to achieve all these objectives, the problem is cast as a repeated online optimization. As the charging power is discontinuous (the minimum charging power is not arbitrarily small), the optimization problem is mixed integer. It also does not require the CS to have precise information about the EVs ramping rates, their state-of-charge (SoC) or actual departure times. The fairness of allocation is performed using the knowledge of desired SoC and expected staying time that the user of an EV advertises upon arrival to the CS.

The main goal in this paper is to evaluate whether the method works in a real environment. The experimental validation has two major challenges. First, we need to verify the real-time capabilities of the method. These characteristics are crucial as the grid state can change rapidly (in few seconds) due to highly volatile energy resources, such as PV plants [11]. In order to cope with this, the control method should be able to work on a sub-second scale. The main issue here is solving a mixed-integer optimization problem in real-time. In [10], a specific heuristic is proposed to reduce the amount of integer variables. Then, the problem is solved using Branch-and-Bound [12]. However, directly solving this problem can

978-1-6654-3597-0/21/$31.00 ©2021 IEEE

Authorized licensed use limited to: Lorenzo Reyes-Chamorro. Downloaded on January 06,2023 at 17:49:28 UTC from IEEE Xplore. Restrictions apply.

take several seconds and a commercial solver code is needed. Alternatively, in this paper we suggest a procedure that solves several strictly convex optimization problems with fixed combinations of integer variables by using open-source software. We show that the method can compute the power setpoints for EVs at sub-second scale. Second, most of the control methods presented in the literature assume that each EV perfectly follows a power setpoint and does not take into account inaccuracies and delays in the implementation of the power setpoint. As this non-ideal behaviour could significantly influence the results, we experimentally assess how fast commercial EVs respond to changes of power setpoints. In this respect, we perform several EVs charging sessions in the presence of a rapidly fluctuating PV production. By taking into account these non-ideal behaviour, we show that the method fairly charges EVs and opportunistically use the available power, while respecting the grid operational constraints.

Our main contributions are the following:

- We experimentally validate a recently proposed charging-control method on a real-scale microgrid with real EVs and show fair allocation of a power among the EVs while tracking an aggregated power-setpoint and minimizing EV battery wear.
- We implement the method and make it compatible with real equipment and existing EV charging standards.
- We confirm that EVs charging can be controlled in real-time via time-varying power setpoints. However, the reaction time to power setpoint change and the implementation accuracy depends on the EV type. In this respect we show that the method is capable to account for these inaccuracies and compensate them.

The structure of the paper is as follows. In Section II, we summarize the charging-control method and explain its implementation. In Section III, we describe the experimental setup. In Section IV, we provide the results of the validation and comparative experiments. Finally, we conclude the paper in Section V.

II. Summary of the EV charging station control architecture

A. Charging-Station Control

In this section, we describe the main principles of the control method proposed in [10]. We consider a CS that can host N EVs. Time is discretized in constant intervals, indexed by k. The CS provides, at each time step k, the measured active charging power $\hat{P}_i[k]$ and reactive power $\hat{Q}_i[k]$ for the i-th connected EV. The CS keeps track of the number of connected EVs $\Gamma[k]$ at every step k. A newly arrived EV cannot start charging before being instructed by the CS. We also assume that, upon arrival, every EV user advertises to the CS the following quantities: (i) charging-power bounds $P_i^{\min}$ and $P_i^{\max}$ (ii) energy demand ΔE_i^{dem}, (iii) the expected departure time k_i^{dep}. At the k-th timestep the CS also receives an aggregated power-setpoint $P^{\text{req}}[k]$ from the grid controller (see Section III-A for more details). The value of $P^{\text{req}}[k]$ accounts for the current capabilities of the various resources in the grid, (such as PVs), as well as the grid constraints.

At time step k, the problem is to decide on the collection $\mathcal{P}[k] = (P_i[k])_{i=1,\dots,\Gamma[k]}$, where $P_i[k] \in \{0\} \cup [P_i^{\min}, P_i^{\max}]$ is the charging power assigned by the CS to slot i at time k and on the collection $\Omega[k] = (\omega_i[k])_{i=1,\dots,\Gamma[k]}$, where $\omega_i[k]$ is the on/off decision for EV i. Specifically, $\omega_i[k] = 1$ (respectively, 0) means that the CS decides to switch EV i on (respectively, off) at time k. We assume that an EV is initially switched off upon arrival. When receiving new setpoints from the CS, the EV cannot immediately change its charging power due to the following delays: *reaction* delay is the time an EV takes, after receiving a new setpoint, to start modifying its power, and *implementation* delay is the time an EV takes to reach a new setpoint, which depends on the EV charger ramping rate. The EV is *locked* if it is in the process of reacting to, or implementing a setpoint. Let $\mathcal{C}[k]$ be the collection of EVs that are unlocked at time k and let $\mathcal{L}[k]$ collect all locked EVs.

The implementation of the method is based on the four-step process described below. First, two non-linear integral terms are computed to account for: (i) the past behaviour of EVs charging power, and (ii) the desire of an EV to be charged. The first of these terms, $\lambda_i[k] \in [0.5, 1]$ per EV i, quantifies how long ago and how large the power changes were. This is used as a priority metric: the smaller λ_i, the higher the priority to change power. The second term, $\rho_i[k] \in [0.5, 1]$, expresses the desire of an EV i to charge. It is also used as a priority metric: the larger ρ_i, the higher the priority to increase power. Let $\Lambda[k] = (\lambda_i[k])_{i=1,\dots,\Gamma[k]}$ and $R[k] = (\rho_i[k])_{i=1,\dots,\Gamma[k]}$.

Second, the method finds the power allocation that maximizes EV energy-demand satisfaction while ensuring fairness, i.e., $P^{\text{req}}[k]$ must be allocated fairly among available EVs. Commonly used fair allocations are weighted proportional and weighted max-min; in [10] it is proved that they are equivalent in our setting. Thus, the method computes, using a water-filling algorithm, the weighted-max-min fair allocation, where the weight of an EV reflects its energy demand and its expected staying time. The result of the step is the collection $\mathcal{P}^{\text{ref}}[k]$ of *reference powers*, $P_i^{\text{ref}}[k] \in [0, P_i^{\max}]$ for all EVs, ideally fair and such that $\sum_{i \in \Gamma[k]} P_i^{\text{ref}}[k] = P^{\text{req}}[k]$.

Third, in order to avoid exponential complexity, the method uses a heuristic that runs at every time k and limits the number of integer variables. The heuristic partitions the set of unlocked EVs into three subsets: EVs that are forced to be switched (or remain) on ($\mathcal{S}^{\text{on}}[k]$), EVs that are forced to be switched (or remain) off ($\mathcal{S}^{\text{off}}[k]$), and EVs for which the on/off decision is decided by the optimization problem ($\mathcal{S}[k]$). It is required that $|\mathcal{S}[k]| \leq m$, m is a fixed small number.

Fourth, the method solves the following mixed-integer optimization problem repeatedly, at every time-step:

$$\textbf{(H)} \quad \min_{\mathcal{P}[k],\Omega[k]} f_0(\mathcal{P}[k], P^{\text{req}}[k]) + (f_1(\mathcal{P}[k], \Lambda[k]) + f_2(\Omega[k], R[k], \hat{\mathcal{P}}[k])) + f_3(\mathcal{P}[k], \mathcal{P}^{\text{ref}}[k]) \tag{1}$$

$$\text{s.t. } P_i^{\min}\omega_i[k] \leq P_i[k] \leq P_i^{\max}\omega_i[k] \tag{2}$$

$$\omega_i[k] \in \{0,1\}, \forall i \in \mathcal{C}[k] \tag{3}$$

$$\omega_i[k] = 1, \forall i \in \mathcal{S}^{\text{on}}[k] \tag{4}$$

$$\omega_j[k] = 0, \forall j \in \mathcal{S}^{\text{off}}[k] \tag{5}$$

Authorized licensed use limited to: Lorenzo Reyes-Chamorro. Downloaded on January 06,2023 at 17:49:28 UTC from IEEE Xplore. Restrictions apply.

The term $f_0(\mathcal{P}[k], P^{\text{req}}[k])$ implements a soft constraint on the aggregated power-setpoint $P^{\text{req}}[k]$. The terms f_1 and f_2 minimize the wear of EV batteries. f_1 penalizes the difference between $P_i[k]$ and the measured power $\hat{P}_i[k]$, as well as changes in the measured power. Let collection $\hat{\mathcal{P}}[k] = (\hat{P}_i[k])_{i=1,\dots,\Gamma[k]}$. f_2 penalizes the EV disconnection caused by the CS (i.e., $P_i[k] = 0$). The term f_3 maximizes EV energy-demand satisfaction while ensuring fairness, by penalizing the deviation between the setpoint and the fair allocation. For more details about the method see [10].

B. Charging-Power Computation

In this subsection, we describe how we implement in real-time the solution of the mixed-integer problem (**H**). In [10], Branch-and-Bound is used. In this paper, we present an alternative approach that does not need a commercial solver.

As mentioned earlier, the number of integer variables in problem (**H**) is less than or equal to m. Let us assume that at time k, the amount of integer variables equals $v \leq m$. Each of these v variables can be either 0 or 1. Thus, there are 2^v combinations of integer variables. For example, if $v = 2$, then the combinations are: $\{[0,0],[1,0],[0,1],[1,1]\}$. Also, if we choose any fixed combination of integer variables, the problem (**H**) becomes a strictly convex quadratic problem where variables are the collection $\mathcal{P}[k]$. We then solve the problem for each fixed combination of integer variables by using the Goldfarb-Idnani active-set dual method [13], the implementation of which is available online. After this, we evaluate the objective function of (**H**) for every combination of integer variables and their corresponding solutions to the (**H**). Finally, the combination that gives a minimal objective function value is the solution to our problem.

III. Experimental Setup

In order to experimentally validate the charging-control method, we have integrated it into an existing experimental setup that consist of: (i) real-scale microgrid and EVs, (ii) microgrid control framework.

A. Microgrid Control Framework

The microgrid is controlled by the COMMELEC system [14]. It is a multi-agent-based framework for real-time control of power grids. It uses a hierarchy of software agents to control a power grid. Each resource is equipped with a resource agent (RA) that is adapted to the technology features of the resource. The agent responsible to control the entire grid is called the Grid Agent (GA). The GA communicates with its RAs by using a common device-independent protocol for message exchange. Each RA advertises an abstract representation (so-called advertisement) of its internal state by using the following format: (1) the PQ profile is the set in the (P, Q) plane (for active and reactive power) that the resource under the control of the RA can deploy, i.e. resource flexibility. (2) The virtual cost $CF(P, Q)$ is a function that evaluates the preference of a resource to stay in a particular zone of the PQ profile. (3) The belief function $BF(P, Q)$ is a set-valued function that accounts for the uncertainty of the resource operation. Specifically, $BF(P, Q)$ returns a convex set that contains all possible setpoints that the resource might implement when it is instructed to apply (P, Q).

The objectives of the GA are to: (i) keep the grid in a feasible state of operation, i.e. such that nodal voltage magnitudes and line currents are in safe bounds, (ii) minimise the costs of the RAs, (iii) meet the power setpoint requested by an upper GA (for example a dispatch plan). To perform this, the GA first needs the advertisements from the resources and the current electrical state of the grid (usually given by a state estimation process). Then the GA computes optimal power setpoints by minimising the sum of the resources cost functions, using a gradient-based method. The GA ensures that the state of the grid will be feasible by estimating the maximum variation of control by using belief functions. Finally, GA sends power setpoints to the RAs. These process is repeated every 100ms to cope with the fastest possible variations of distributed resources (see [14] for further details).

B. Real-Scale Microgrid and EVs

We validate our method on an implementation of the CIGRÉ benchmark low-voltage microgrid [15], shown in Fig.1. The microgrid interconnects various resources that, for this specific experiment, are composed of a 20kW uncontrollable PV and CS that can simultaneously charge 2 EVs. The CS uses the IEC 61851 standard to communicate with EVs [16]. We use two commercially available EVs: a Tesla Model S 90D (90 kWh Li-Ion battery) and a Renault Zoe (54.7 kWh Li-Ion battery) both equipped with three-phase chargers.

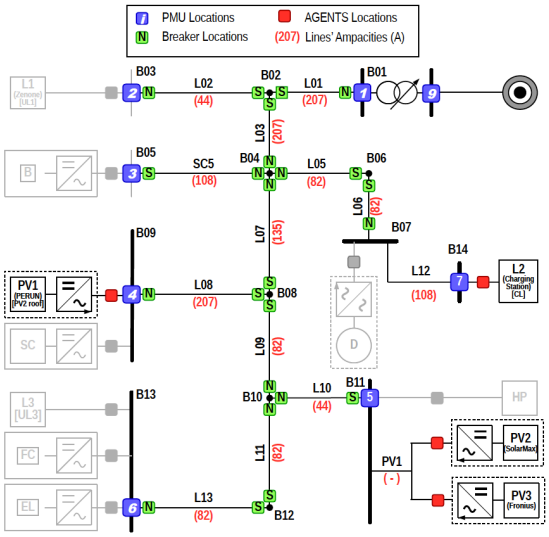

Fig. 1: The experimental microgrid. All elements used in the experiments of this paper are shown in black.

C. Charging Station Agent

In our setting, the charging station is controlled by the GA. For this purpose, it must be equipped with a RA that receives the aggregated power-setpoint (P^{req}) from the GA. Then, it first allocates this power among connected EVs. In order to do so, it uses the method that computes charging powers for all connected EVs (see in Section II). The CS can only control the maximum current I of and EV. Thus, we

Authorized licensed use limited to: Lorenzo Reyes-Chamorro. Downloaded on January 06,2023 at 17:49:28 UTC from IEEE Xplore. Restrictions apply.

need to convert a power setpoint to a current setpoint. We experimentally discover that charging patterns for the adopted EVs are significantly different. In order to investigate such differences, we perform two independent charging sessions of both EVs. We increment the maximum charging current magnitude (I) starting from 6A with steps equal to 0.1A and measure implemented current and voltage fundamental frequency phasors ($\hat{I}$ and $\hat{V}$ respectively), active power $\hat{P}$ and power factor $\cos\phi$ per EV. We show in Fig.2 results of the experiment for Tesla and Renault. We observe that, for the Tesla EV, there is a gap between $\hat{P}$ and $\hat{V}I$ equal to 700W approximately. Also, $\cos\phi$ is always close to 1. For the Renault EV, we see that when charging power is more than 12kW the behavior is similar to the Tesla EV, i.e., $\cos\phi$ is close to 1. However, when power is less than 12kW the Renault EV reactive power is not equal to 0 due to its controller. It means that for some EV chargers, in our case the Renault EV, $\cos\phi$ can be much lower than 1. Thus, in order to provide high fidelity active power tracking, we created two lookup tables for both EVs that map the current setpoint to the corresponding consumed power. Additionally, it is visible that sometimes the Renault EV drops its charging power to 0 and goes back (for example at time close to 1000s) these jumps take around 2s and are caused by the internal controller of this EV.

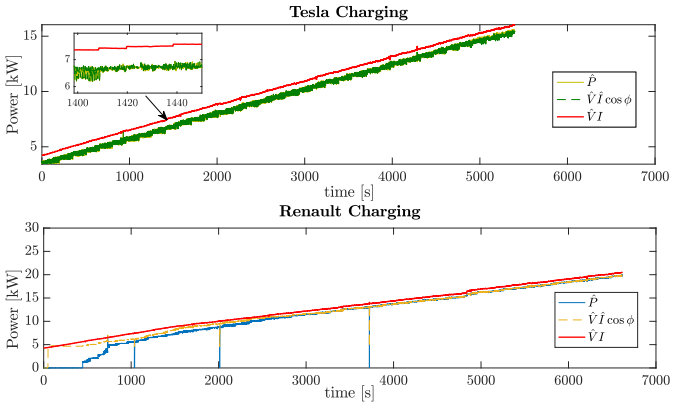

Fig. 2: Tesla and Renault charging patterns.

Since we are using the COMMELEC framework, the agent sends to the GA an advertisement that contains the representation of the CS internal state: (P, Q) profile, virtual cost function $CF(P, Q)$ and belief function $BF(P, Q)$ (see Fig.3). The sending/receiving message cycle is repeated continuously and endlessly. As every EV has its own flexibility and uncertainty, the charging station should be able to advertise the aggregated information. The presence of delays influences the flexibility of the EV; this should be taken into account in the aggregated flexibility.

1) PQ Profile: The locking of EVs reduces the flexibility of the charging station, as it is not permitted to change the charging power of locked EVs. Hence, the amount of power that the charging station will consume, if we switch off all unlocked EVs, is computed as:

$$P^{lb} = \sum_{i \in \mathcal{L}[k]} P_i[k] \tag{6}$$

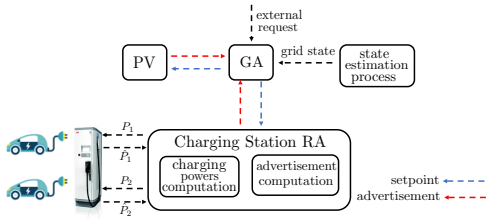

Fig. 3: Overall architecture of the system.

At the other extreme, the amount of power that a charging station will consume if all unlocked EVs consume their maximum power is computed as:

$$P^{ub} = \max\left(\hat{P}[k] + \sum_{i \in \mathcal{C}[k]} (P_i^{\max} - \hat{P}_i[k]), P_{\text{CS}}^{\max}\right) \tag{7}$$

where $P_{\text{CS}}^{\max}$ is charging station rated power and $\hat{P}[k] = \sum_{i \in \Gamma[k]} \hat{P}_i[k]$. Hence, we compute the feasible operation set as $\mathcal{A} = \{(P, Q) | P^{lb} \leq P \leq P^{ub}, Q = \sum_{i \in \Gamma[k]} \hat{Q}_i[k]\}$.

2) Virtual Cost: In this work, the agent prefers to charge the EVs as fast as possible. Therefore, we define the virtual cost function as: $\mathcal{C}(P, Q) = \frac{1}{(P_{\text{CS}}^{\max})^2} P^2 + \frac{2}{P_{\text{CS}}^{\max}} P$.

As we do not control the reactive power of EVs, Q does not appear in the definition of the cost.

3) Belief Function: One of main sources of uncertainty is related to the EV delay on the implementation of the power setpoint, as a setpoint is not implemented immediately, due to the ramping constraints of the battery. When an EV is unlocked, the expected implemented power remains the measured power, on the contrary, when an EV is locked, the implemented power is expected to lie in the range defined by the measured power and the setpoint. Most of the time, the EV implements the instructed power setpoint accurately (see Section IV). However, if the battery of EV i is almost charged (this depends on the EV; in our experiments it occurs around 95% and 90% charge for the Tesla and Renault EVs respectively), it starts to decrease the maximum charging power with a rate Δr_i. The CS has no information about the EVs' SoC, also the Δr_i depends on the type of the battery and its internal conditions. Hence, Δr_i should be estimated dynamically. In this paper, we use a Holt-Winters (double exponential weighted moving average) fitter for Δr_i estimation [17]. The computation of uncertainty bounds $\mathcal{B}_i^{\text{low}}, \mathcal{B}_i^{\text{up}}$ per EV i is detailed in Alg.1. We detect at line 1 if the EV follows the previously computed setpoint. If not, we check if the EV itself reduces its charging power (line 2) by comparing the measured power between two consecutive time steps and update the Δr_i using Holt-Winters estimation (line 3). As a result, we compute the uncertainty bounds in lines $6-10$. Finally, the belief function is computed as aggregated uncertainty of all EVs as $\mathcal{B}(P, Q) = \{\sum_{i \in \Gamma[k]} \mathcal{B}_i^{\text{low}} \leq P \leq \sum_{i \in \Gamma[k]} \mathcal{B}_i^{\text{up}}, Q = \sum_{i \in \Gamma[k]} \hat{Q}_i[k]\}\}$.

The RA for CS is implemented in C++ and cross-compiled for embedded platform and deployed in a NI CRIO 9068.

IV. Experimental Results

The results described in this section refer to the application of the charging control method in a real environment: real

Authorized licensed use limited to: Lorenzo Reyes-Chamorro. Downloaded on January 06,2023 at 17:49:28 UTC from IEEE Xplore. Restrictions apply.

Algorithm 1 Belief function computation for EV i.

Input: $\hat{P}_i[k-1], \hat{P}_i[k], P_i[k-1], P_i[k]$
Output: $\mathcal{B}_i^{\text{low}}, \mathcal{B}_i^{\text{up}}$

if $P_i[k-1] > \hat{P}_i[k]$ **then**
  if $\hat{P}_i[k-1] > \hat{P}_i[k]$ **then**
    $\Delta r_i = Holt - Winters(\Delta r, \hat{P}[k-1] - \hat{P}[k])$
  end if
end if
if $P_i[k] >= \hat{P}_i[k-1]$ **then**
  $\mathcal{B}_i^{\text{low}} = \hat{P}_i[k] - \Delta r_i, \mathcal{B}_i^{\text{up}} = P_i[k]$
else
  $\mathcal{B}_i^{\text{low}} = P_i[k] - \Delta r_i, \mathcal{B}_i^{\text{up}} = \hat{P}_i[k]$
end if

EVs and real-scale microgrid. Several scenarios are considered in order to demonstrate the performance of the method. We use the root mean square error (RMSE) as a metric to measure how good the CS follows the PV production. For the fairness and battery wear per EV i we use metrics from [10]: (i) non-satisfied demand $M_i^{\text{nsd}} = 1 - \Delta E_i / \Delta E_i^{\text{dem}}$, where ΔE_i is the energy that EV i receives while plugged-in, (ii) battery-wear $M_i^{\text{bw}} = \frac{1}{2(P_i^{\max})^2} \sum_{k=1}^{K} (P_i[k] - P_i[k-1])^2$, where K is the amount of discrete time-steps during the selected control period.

A. Self-consumption scenarios

We first study the performance of the proposed method when the grid state is far from the operational limits in terms of bus voltages and line ampacity constraints. The GA is instructed to track 0kW at the PCC, i.e. the grid should be self consuming as much as possible. In this case, the CS should follow the fluctuating PV production. In order to validate the performance of our method, we create two scenarios: (i) *Scenario* 1, where both EVs have the same expected staying time (1h 40min) and energy demand (15kWh), in this case our method should charge both EVs similarly. (ii) *Scenario* 2 where Renault and Tesla EVs have similar energy demand (10kWh and 11kWh respectively), but the Renault EV has smaller expected staying time (45min for the Renault EV and 1h 10min for the Tesla EV). Additionally, the Renault EV arrives and departs while the Tesla one is plugged-in. In this case, the Renault EV should receive more power than the Tesla EV while plugged-in because it has higher priority to charge. It should be noticed that in both scenarios the PV production is not enough to satisfy EVs charging demands fully. Additionally, in both scenarios EVs depart earlier than expected, i.e. disconnection is caused by a decision of a user.

The results for Scenario 1 are shown in Fig.4. It is visible that CS power perfectly follows the PV production and PCC power is always close to 0. The RMSE value between PCC target power (i.e., 0kW) and the realized one is 254W. Tesla and Renault EVs share PV fluctuations, charge almost at the same power due to the equal priority and receive 6.75kWh ($M^{\text{nsd}} = 0.55$) and 6.81kWh ($M^{\text{nsd}} = 0.55$) respectively at departure. Also, the EVs accurately follow setpoints due to implemented lookup tables that are explained in Section III-C. Battery-wear metrics for both EVs are also less than 1, meaning that there were no large jumps of the charging power: 0.012 for the Tesla EV and 0.091 for the Renault EV. Finally, we observe two power jumps for the Renault EV around $t =$ 1800s and $t = 3500$s, the possible reasons are discussed in Section III-C.

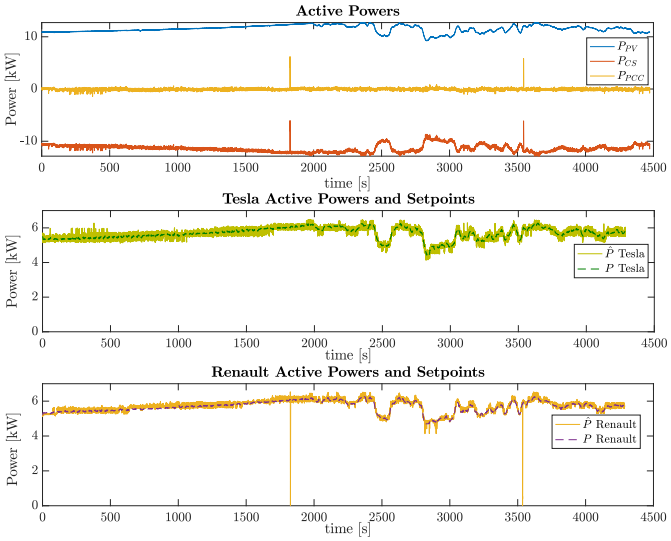

Fig. 4: Scenario 1 experimental results.

The results for Scenario 2 are shown in Fig.5. We observe that, first, the Tesla EV follows the PV production with high fidelity. Then, the Renault EV arrives around $t = 750$s and start charging. After several seconds the Renault EV charges with higher power since it has more priority due to short staying time and similar energy demand. We also see that both EVs follow the PV production and share its fluctuations. The Renault EV stays around 30min and departs at around $t = 2550$s. Tesla and Renault EVs receive 2.64kWh ($M^{\text{nsd}} = 0.73$) and 4.14kWh ($M^{\text{nsd}} = 0.58$) respectively during the Renault EV plugged-in time. Finally, the disconnection of the Renault EV causes a jump of the power. The reason is that, upon disconnection, the power consumed by the Renault EV suddenly goes to 0kW, whereas the Tesla EV cannot immediately react to power change and need several seconds (around 4s) to increase its consumption. After that, the Tesla EV follows the PV production perfectly. The final RMSE value between PCC target power (i.e., 0kW) and the realized one is 448W. In this experiment we also see the power jump caused by Renault internal behavior ($t = 2550$s). Battery-wear metric 0.006 for the Tesla EV and 0.004 for the Renault EV, i.e, there were no large jumps of the charging power.

B. Line congestion scenario

In order to study the behavior of the method under binding-grid conditions, we consider a scenario in which the ampacity of the line connecting the CS and the grid (line L12 in Fig.1) is artificially limited to 23A. In this case, the GA main priority is to keep the grid in a feasible operation and prevent voltage and/or current violations by curtailing the CS consumption (see [14] for details on how the GA enforces grid constraints).

Authorized licensed use limited to: Lorenzo Reyes-Chamorro. Downloaded on January 06,2023 at 17:49:28 UTC from IEEE Xplore. Restrictions apply.

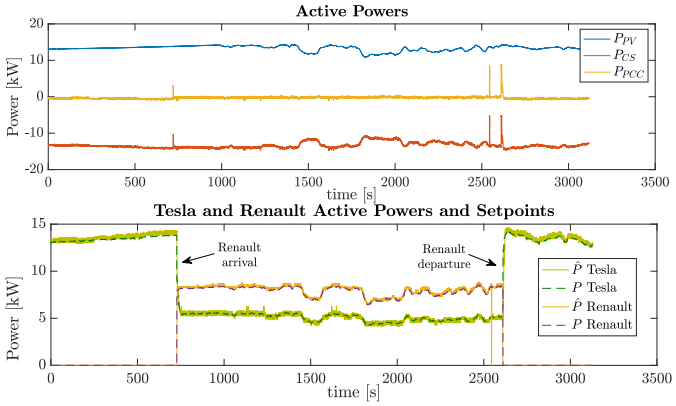

Fig. 5: Scenario 2 experimental results.

In this scenario both EVs stay connected for 45min, but the energy demand of the Tesla EV is of 15kWh, whereas for the Renault EV is of 10kWh.

Fig.6 shows power traces, current at line L12 and EVs active power and setpoints. The line congestion management is clear around $t = 1000$s, the CS follows increasing PV production, however, given the congestion in L12, the consumption of CS is temporarily reduced by the GA and allows CS to consume only 15kW. We observe also that the method reduces the consumption of both EVs, while keeping priority for the Tesla. Both EVs receive 6.62kWh ($M^{\text{nsd}} = 0.55$) and 4.37kWh ($M^{\text{nsd}} = 0.55$) respectively. Additionally, the results show that our control method allows the GA to fully exploit the flexibility of EVs. In this experiment we also see the spurious jump of the Renault EV charging power approximately at $t = 950$s and $t = 2750$s.

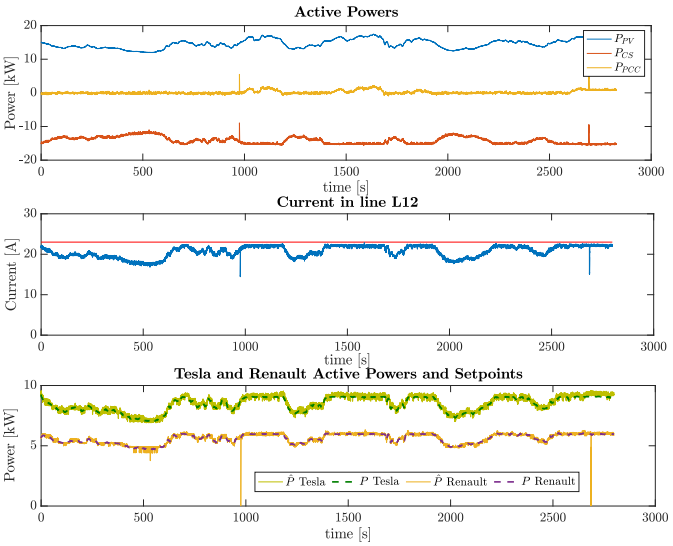

Fig. 6: Line congestion experimental results.

V. Conclusions

In this paper we have experimentally validated the operation of a recently proposed real-time control method for charging EVs. We have performed field validation on a real-scale microgrid with real PV production and two commercially available EVs: a Tesla Model S 90D and a Renault Zoe. We have conducted several field experiments with different PV production, EVs energy desires and staying times. We have showed that the method is able to provide a real-time control (i.e., at sub-second scale) for charging commercial EVs. The results have also showed that the CS is able to accurately follow an aggregated power-setpoint and capable to satisfy the grid operational constraints. The method has allocated the power among EVs fairly charging an EV with higher charging priority and minimising the battery wear. We have also studied charging patterns of EVs.

References

[1] G. Putrus, P. Suwanapingkarl, D. Johnston, E. C. Bentley, and M. Narayana, "Impact of electric vehicles on power distribution networks," *IEEE Vehicle Power and Propulsion Conference*, 2009.

[2] N. B. G. Brinkel, I. Lampropoulos, and W. AlSkaif, T.A. van Sark, "Should we reinforce the grid? Cost and emission optimization of electric vehicle charging under different transformer limits," *Applied Energy*, vol. 276, 2020.

[3] G. Wenzel, M. Negrete-Pincetic, D. Olivares, J. MacDonald, and D. Callaway, "Real-time charging strategies for an electric vehicle aggregator to provide ancillary services," *IEEE Transactions on Smart Grid*, vol. 9, no. 5, pp. 5141–5151, March 2017.

[4] J. Quiros-Tortos, L. Ochoa, S. Alnaser, and T. Butler, "Control of EV charging points for thermal and voltage management of LV networks," *IEEE Transactions on Power Systems*, vol. 31, no. 4, pp. 3028–3039, July 2016.

[5] J. Hu, S. You, M. Lind, and J. Ostergaard, "Coordinated charging of electric vehicles for congestion prevention in the distribution grid," *IEEE Transactions on Smart Grid*, vol. 5, no. 2, pp. 703–711, March, 2014.

[6] E. L. Karfopoulos and N. D. Hatziargyriou, "A multi-agent system for controlled charging of a large population of electric vehicles," *IEEE Transactions on Power Systems*, vol. 28, pp. 1196–1204, May, 2013.

[7] S. Martinenas, K. Knezovic, and M. Marinelli, "Management of power quality issues in low voltage networks using electric vehicles: experimental validation," *IEEE Transactions on Power Delivery*, vol. 32, pp. 971–979, April, 2017.

[8] M. Marinelli, S. Martinenas, K. Knezovic, and P. B. Andersen, "Validating a centralized approach to primary frequency control with series-produced electric vehicles," *Journal of Energy Storage*, vol. 7, pp. 63–73, 2016.

[9] K. Knezovic, S. Martinenas, P. B. Andersen, A. Zecchino, and M. Marinelli, "Enhancing the role of electric vehicles in the power grid: field validation of multiple ancillary services," *IEEE Transactions on Transportation Electrification*, vol. 3, pp. 201–209, March, 2017.

[10] R. Rudnik, C. Wang, J. Reyes-Chamorro, Lorenzo Achara, J.-Y. Le Boudec, and M. Paolone, "Real-time control of an electric-vehicle charging station while tracking an aggregated power-setpoint," *IEEE-Trans. on Industry Applications*, vol. 56, no. 5, pp. 5750 – 5761, 2020.

[11] D. Torregrossa, J.-Y. Le Boudec, and M. Paolone, "Model-free computation of ultra-short-term prediction intervals of solar irradiance," *Solar Energy*, vol. 124, pp. 57–67, Feb. 2016.

[12] F. S. Hillier and G. J. Lieberman, *Introduction to Operations Research*. McGraw-Hill, 2010.

[13] D. Goldfarb and I. A., "A numerically stable dual method for solving strictly convex quadratic programs." *Mathematical Programming*, no. 27, pp. 1–33, 1983.

[14] A. Bernstein, L. Reyes-Chamorro, J.-Y. Le Boudec, and M. Paolone, "A composable method for real-time control of active distribution networks with explicit power set points. Part I: Framework," *Electric Power Systems Research*, vol. 6, pp. 254–264, August, 2015.

[15] Taskforce C6.04.02, "Benchmark Systems for Network Integration of Renewable and Distributed Energy Resources," CIGRÉ, Tech. Rep., 2010.

[16] IEC 61851-1, "International standard."

[17] J.-Y. Le Boudec, *Performance Evaluation of Computer and Communication Systems*. EPFL Press, Lausanne, Switzerland, 2010.

Authorized licensed use limited to: Lorenzo Reyes-Chamorro. Downloaded on January 06,2023 at 17:49:28 UTC from IEEE Xplore. Restrictions apply.